

Projectile charge-state dependence of K x-ray production by 1–4-MeV/amu heavy ions in gases*

J. Richard Mowat, I. A. Sellin, P. M. Griffin, D. J. Pegg, and R. S. Peterson

Department of Physics and Astronomy, University of Tennessee, Knoxville, Tennessee 37916

Oak Ridge National Laboratory, Oak Ridge, Tennessee 37830

(Received 18 June 1973)

We report the observation of large projectile-structure effects in heavy-ion-induced K x-ray yields from thin, light gas targets in a projectile energy region ($\sim 1\text{--}4$ MeV/amu) where molecular promotion effects are not expected to be significant. The K x-ray yield from both projectile and target is found to be very sensitive to the ionic charge q of the projectile. In some cases, notably for Ar^{q+} on Ne at 80 MeV and for Cl^{q+} on Ne at 42 MeV, the target yield increases exponentially with projectile charge, the projectile nuclear charge and velocity remaining constant. In all cases, the projectile K x-ray yield increases faster than exponentially, even when the incident projectile has a full K shell. It is evident that targets become highly ionized in these collisions, and already highly ionized projectiles are often further ionized in these targets of less-than-equilibrium thickness. We discuss the limitations imposed on the determination of absolute x-ray cross sections in multiply ionizing collisions. These limitations cast serious doubt on the accuracy of K -shell ionization cross sections extracted from measured K x-ray cross sections in this and other experiments. The projectile-target combinations studied in the present experiment are Ar^{q+} on Ne (at 80 and 152 MeV), Cl^{q+} on Ne and SF_6 (at 42 and 50 MeV), and F^{q+} on two chlorine-bearing Freon compounds (at 43 MeV).

I. INTRODUCTION

When highly stripped ions penetrate matter, multiple excitations commonly occur in both the projectile and the target atoms. Among the possible processes is K -shell ionization, and K x rays are generally observed coming from both collision partners. Theories of inner-shell Coulomb ionization by fully stripped ions assume that the projectile is a point charge, i.e., without structure. These theories^{1,2} predict, on very general grounds, that for different projectiles incident on the same target at the same velocity, the ionization cross section should be quadratic in the projectile nuclear charge Z . Deviations from this Z^2 dependence have recently been observed,³ the actual cross section being found to increase faster than Z^2 .

In this paper we report the results of a different type of inner-shell ionization experiment. For projectile energies in the region 1–4 MeV/amu we have studied target and projectile K x-ray yields in gas targets as a function of the ion charge, with projectile nuclear charge, projectile velocity and initial target state remaining fixed. The most significant result is that the x-ray cross section is a strong function of the charge on the incoming ion. In many cases the x-ray yield increases exponentially as the projectile charge state is increased one step at a time. The experiment is not intended to measure the energy of the emitted x ray precisely enough to determine the exact electronic configuration (and thereby

infer the fluorescence yield) of the emitting ion. However, it does reveal that when the projectile ion contains fewer than two electrons, the target atom is sometimes very highly ionized, and x rays whose energies correspond to transitions between one-electron target states are observed.⁴ Lacking knowledge of the specific states formed, their fluorescence yields, and their relative populations, we quote our results as total K x-ray production cross sections rather than as ionization cross sections. A summary of the various experimental systems studied is given in Table I. Similar experiments have recently been reported by other investigators. They involve K and L x-ray production in argon, krypton, and xenon induced by 35.7-MeV fluorine ions⁵ (target data only), and Al K x-ray production induced by 12–68-MeV oxygen ions⁶ (solid target).

II. DESCRIPTION OF EXPERIMENTS

Beams of Ar, Cl, and F in single charge states and in the energy region 1–4 MeV/amu pass through a thin gas target, and the x rays emitted are detected in a lithium-drifted silicon diode. Table I summarizes the variety of beam species, beam energies, projectile charge states, and target gases that were used in the experiments. The argon beams were obtained from the Oak Ridge Isochronous Cyclotron. Currents through the gas cell ranging from a few nanoamperes for the most probable charge states to a few tens of picoamperes for the more inaccessible states gave re-

TABLE I. Summary of experimental systems.

Projectile	Energy (MeV)	Velocity (10^9 cm/sec)	Charge state	Target	Target K velocity (10^9 cm/sec)	K x-ray yields studied
$^{40}\text{Ar}^{q+}$	152	2.70	8, 14, 15, 16, 17, 18	Ne	1.75	Ne, Ar
	80	1.96	6, 12, 13, 14, 15, 16	Ne	1.75	Ne, Ar
$^{35}\text{Cl}^{q+}$	50	1.66	11, 12, 13, 14	Ne	1.75	Ne, Cl
	42	1.09	10, 11, 12, 13, 14, 15	Ne SF_6	1.75 1.55 (F)	Ne, Cl F
$^{19}\text{F}^{q+}$	43	2.09	7, 8, 9	ClCF_3	3.15 (Cl)	Cl
				Cl_2CF_2	3.15 (Cl)	Cl

peatable results. The chlorine and fluorine beams were produced by the 7-MV tandem van de Graaff accelerator at ORNL. After extraction from the accelerator the primary beam (typical charge state +6 to +8) is passed through a thin carbon foil ($10\text{--}40 \mu\text{g}/\text{cm}^2$) which further ionizes the beam particles and distributes them among a variety of charge states. Out of these a single state is selected magnetically and deflected through the gas target. The beam is tightly collimated before entering the differentially pumped gas cell to ensure that none of the beam strikes the cell walls and that all of the beam viewed by the Si (Li) detector is intercepted by the downstream Faraday cup used for particle normalization. The Faraday cup is both electrically and magnetically guarded to avoid spurious current measurements from secondary and stray electrons.

A. Targets

The targets are confined to a region of length ~ 1 cm along the beam direction by differential pumping apertures. Gas pressure is measured using a capacitance manometer. An amplified feedback signal obtained from the manometer drives a servomechanical leak valve which establishes the gas flow to the cell and thereby regulates the target pressure. The manometer was checked by comparing it with a McLeod gauge and found to be accurate to within 1 mTorr in the region near 20 mTorr. The pressure determination introduces a 5% uncertainty in our cross-section measurements, most of which were taken at 20 mTorr. This target pressure was chosen to maximize the x-ray yield while still maintaining approximately single-collision conditions.

A gas target is considered "thin" if a projectile makes, on the average, less than one collision

while passing through the target. Since different kinds of collision processes present different sized cross sections to the projectile, a target

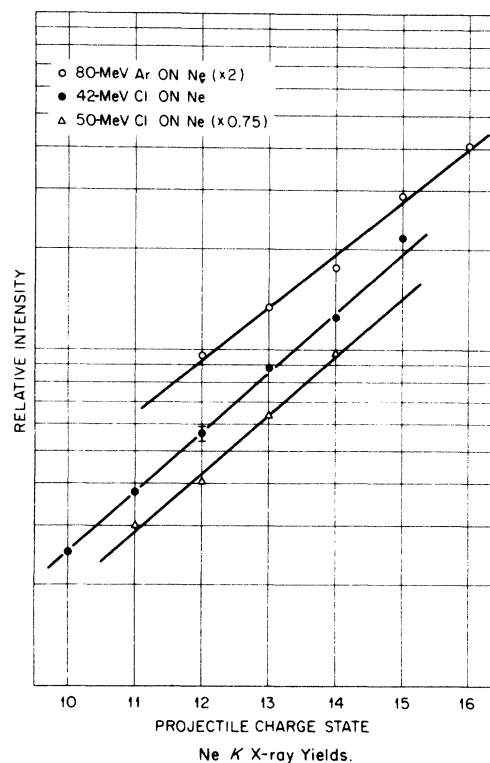


FIG. 1. Relative yields of neon K x rays induced by highly stripped argon and chlorine ions plotted against projectile charge state. Unless otherwise indicated by error bars, the point size overestimates the combined uncertainty arising from counting statistics and pressure measurement. The curves are single exponential fits to the experimental points. Note the normalization factors used to avoid the overlapping of curves that would otherwise occur.

may be thin for some processes and thick for others. In the velocity region considered here, the largest relevant effect that occurs is the capture of a target electron by a projectile ion. Since this process alters the initial charge state of an incident projectile, it is important that such a projectile not make a subsequent *K*-shell ionizing collision. Furthermore, since electron capture contaminates the charge-state purity of the beam, the capture rate must be kept so low that it does not cause serious error in the conversion from electrical current to particle current. Assuming an electron-capture cross section $\leq 1 \times 10^{-16} \text{ cm}^2$ for these projectiles at these velocities, only seven out of 100 ions undergo electron capture in a 1-cm-long gas cell at room temperature and at 20-mTorr pressure. Target operation at 20 mTorr then ensures approximately single-collision conditions. The projectile charge state going into a collision depends upon whether or not the ion has made a prior charge changing collision. This is a matter of importance since, if the *K*-shell ionization cross section depends upon the projectile charge, then the yield will not be linear in pressure if the gas is sufficiently dense that an appreciable number of projectiles change charge prior to the ionizing collision. Linearity of x-ray yield versus pressure was checked for Ar^{16+} and Ar^{14+} beams at pressures up to 25 mTorr. Least-squares fits to the data passed through the origin within the 1-mTorr pressure-setting accuracy, and these fits revealed no evidence for systematic curvature. We take the apparent linearity of these curves as evidence that single collisions prevail in the target.

B. Detector

X rays produced by collisions in the gas cell are detected in a lithium-drifted silicon diode (ORTEC model 7116, sensitive volume is $12.6 \text{ mm}^2 \times 3.31 \text{ mm}$). The detector views an effective length of 0.42 cm of gas. X rays that are absorbed in the sensitive volume produce electrical pulses which are amplified, shaped, and stored in the standard manner, according to pulse height in a multichannel analyzer. Noise in the sensitive volume and in the amplifier causes an approximately Gaussian distribution of pulse heights about the mean value. The total system resolution contains an energy-independent part which is a function of preamplifier noise and amplifier time constants and an energy-dependent part from ionization statistics in the Si(Li) diode. The analyzer thus represents a monoenergetic x-ray spectrum as a Gaussian peak whose center corresponds to the x-ray energy and whose width is $\leq 200 \text{ eV}$ at 1 keV. This system

resolution is sufficient to distinguish between target and projectile x rays in all cases studied in this experiment. The resolution is not fine enough to distinguish between all the possible *K* x rays associated with different electronic configurations of the emitting ion. Nevertheless, as discussed below, we do obtain useful information concerning the extent of target ionization.

The detector energy calibration is performed in two steps. Detector pulses from x rays of known energy (e.g., $\text{MnK}\alpha$, $K\beta$ at 5.894 keV, and 6.49 keV, respectively, emitted when ^{55}Fe decays by *K* capture) are compared in pulse height with electronically simulated pulses generated by a calibrated linear pulser (ORTEC model 731). These simulated pulses are applied at the preamplifier input in place of detector output pulses. This comparison serves to check the manufacturer's calibration of the linear pulser. This calibration was found to be entirely satisfactory as regards both absolute setting accuracy and linearity. The pulser is then used to calibrate the detector over the region of interest.

In order to deduce absolute cross sections from the detected x-ray yields corrections must be

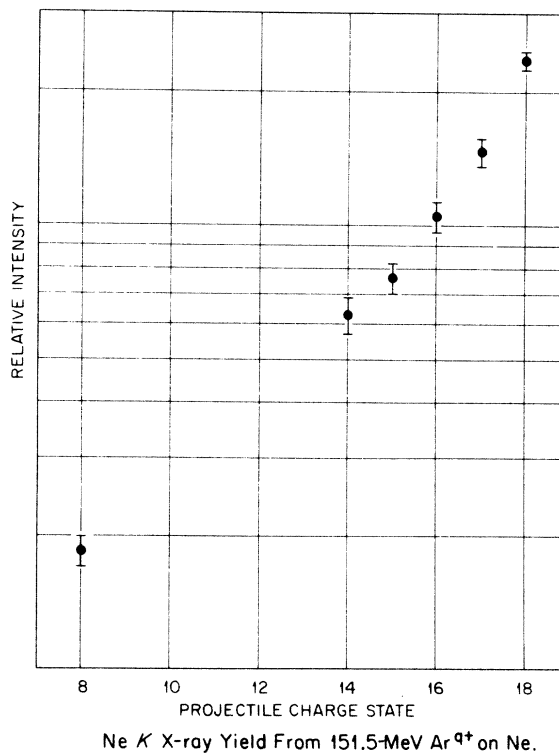


FIG. 2. Relative yields of neon *K* x rays induced by 151.5-MeV Ar^{q+} on neon. The error bars reflect the combined uncertainty arising from counting statistics and pressure measurement.

applied to account for x-ray intensity losses in the detector. These losses arise principally from photoionization in the three layers through which all detected x rays must pass: (i) a 0.0005-in. beryllium window which seals the evacuated detector housing, (ii) a 200-Å gold layer which serves as the ionization-charge collector and (iii) a ~1 μm "dead" layer in which charge collection is inhibited at the boundary of the sensitive volume. An estimate of the over-all photon transmission

$$T \equiv I/I_0 = \exp\left(-\sum_i \mu_i \rho_i t_i\right) = \exp\left(-\sum_i \frac{\sigma_i}{M_i} \rho_i t_i\right)$$

can be made if the thickness t_i , density ρ_i , and mass attenuation coefficient μ_i (or photoionization cross section σ_i and atomic mass M_i) are known and assumed uniform throughout each layer. In general, the transmission is x-ray energy dependent on account of the energy dependence of the photoionization cross section. The total x-ray transmission through the three layers is an exponential function of nine quantities, so the accuracy of the estimated transmission is strongly dependent upon the uncertainties associated with them. With the exception of the Be and Si densi-

ties, none of these nine quantities is known⁷ to better than ~10%. For this reason we assign an uncertainty of a factor of 2 to the estimated detector transmission at any energy in the 700–1000-eV range, where the transmission is estimated to range between 0.02 and 0.20. The principal uncertainty arises from the uncertainties in the beryllium window thickness and the gold layer density.⁸ If these were known exactly, the absorption could be estimated to within 20%. The absorption uncertainties are much reduced for the 3-keV argon *K* radiation because the absorption itself is much smaller and less strongly dependent upon x-ray energy in that region than in the 700–1000-eV region. (At 3 keV the estimated absorption is no worse than 15%.)

III. EXPERIMENTAL RESULTS

The results of this experiment are presented in Figs. 1–6, which show that, in all cases studied, *K* x-ray production from both target and projectile is strongly dependent upon the charge state of the projectile. With the exception of the data from 80-MeV argon on neon collisions⁴ (Figs. 1 and 5) none of these results has been previously published. Smaller but otherwise similar trends have been reported⁵ recently for target *K* x rays excited

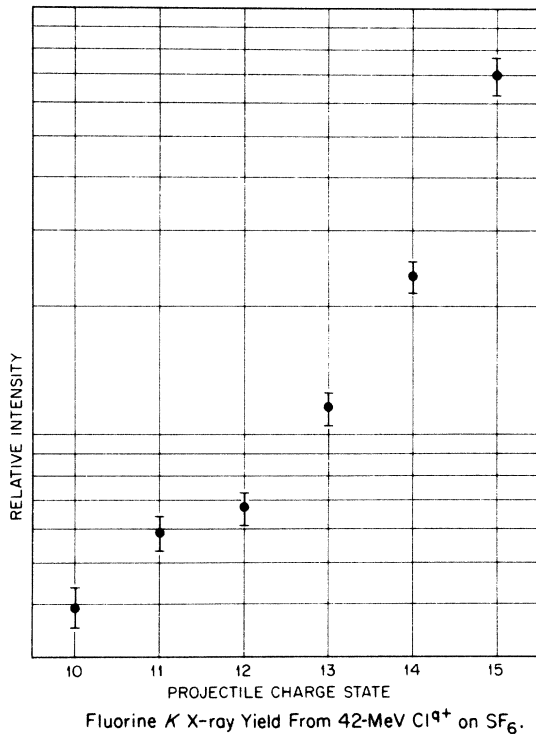


FIG. 3. Relative yields of fluorine *K* x rays induced by 42-MeV Cl⁹⁺ on SF₆. The error bars reflect the combined uncertainty arising from counting statistics and pressure measurement.

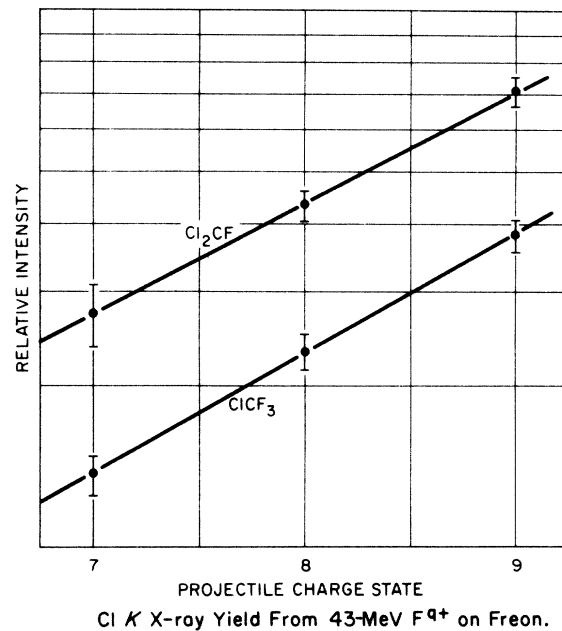


FIG. 4. Relative yields of chlorine *K* x rays induced by 43-MeV F⁹⁺ on two types of chlorine-bearing Freon. The curves are linear least-squares fits to the experimental points. The error bars represent the combined uncertainty arising from counting statistics and pressure measurement.

by 37.5-MeV fluorine on argon. In some cases, notably for neon and Freon targets (Figs. 1 and 4), the target yield increases exponentially with increasing projectile charge state. In all cases (Figs. 5 and 6) the projectile K x-ray yield increases faster than exponentially with increasing charge state.

Each point on each plot represents the number of K x rays actually counted normalized to an arbitrary number of incident particles and gas pressure. The error bars shown represent the combined uncertainties from pressure measurement and x-ray counting statistics (the error due to particle counting statistics is negligible).

These figures are intended to demonstrate the *relative* yield for a particular target as a function of projectile charge state. Detector solid angle and window absorption correction factors have not been applied to these data since these two corrections are the same for all data points taken with a particular target assuming the target radiation spectrum is independent of projectile charge state. This assumption is only approximately true since the cross section for multiple ionization (and therefore the radiating configuration and x-ray

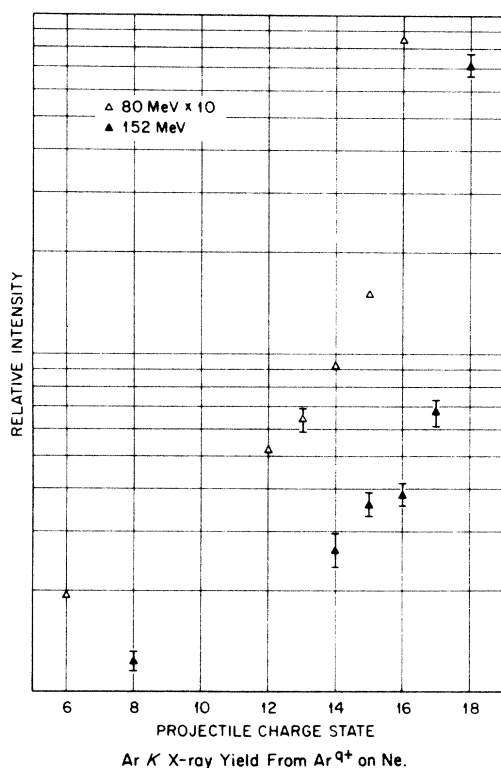


FIG. 5. Relative yields of argon K x rays from Ar^{q+} collisions in neon. The error bars represent the combined uncertainty arising from counting statistics and pressure measurement.

energy) probably depends somewhat on the projectile charge. However, within the resolution of our detector, we do not discern any systematic centroid shifts with increasing projectile charge state except for Ar^{16+} , Ar^{17+} , and Ar^{18+} , even though such shifts should be *enhanced* by the energy dependence of the window transmission factor. In the cases where such energy shifts are noted (Fig. 2) the target x-ray production curve rises more steeply than does a single exponential.

Some particular features of these data are worth noting. The x-ray production curves obtained with 42- and 50-MeV chlorine ions incident on neon (Fig. 1) overlap within counting statistics. For that projectile-target system, at those energies, neither the slope of the curve nor the absolute cross section are strong functions of projectile

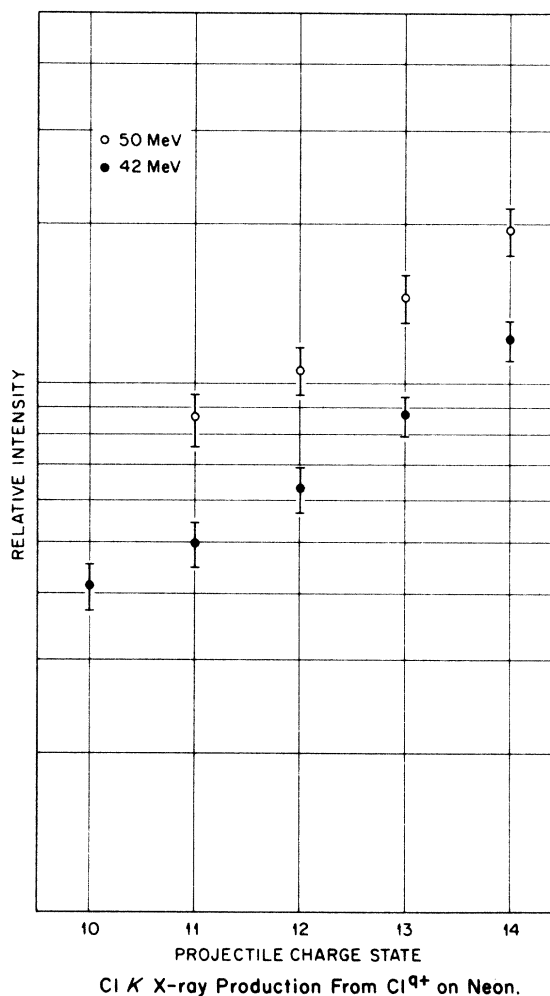


FIG. 6. Relative yields of chlorine K x rays from Cl^{q+} collisions in neon. The error bars represent the combined uncertainty arising from counting statistics and pressure measurement.

energy. The yields of Cl K x rays obtained by bombarding two different Freon targets (Fig. 4) with 43-MeV fluorine agree, within overlapping experimental errors, with the Ar K x-ray yields obtained in Ref. 5 by bombarding argon with 35.7-MeV fluorine.

The experimental results are further summarized in Tables II–V, where we quote the absolute K x-ray production cross sections $\sigma_x = \sigma_{\text{ion}}^K(q)\bar{\omega}_K$, as a function of projectile charge q , which are derived from our measured x-ray yields, as corrected for detector-absorption and solid-angle factors. Errors accompanying entries in the table include the uncertainties in pressure measurement and photon counting, but do not include the uncertainty in window-transmission estimates. Even if the window-transmission factor were known exactly at all energies, there would still be an uncertainty in the x-ray absorption, because the transmission factor is energy dependent, and the precise energy spectrum of the detected x rays is not known. We estimate that the entries in these tables might be in error by as much as a factor of 2 for the lowest energy x rays owing to uncertainties in the window transmission. For the higher energy x rays near 3 keV, this uncertainty is reduced to ~15%.

The ionization cross section $\sigma_{\text{ion}}^K(q)$ cannot be separated from the x-ray cross section σ_x unless the effective fluorescence yield $\bar{\omega}_K$ is known. The appropriate ω_K have been computed for all possible K -, L -, and M -shell defect configurations in neon.⁹ However, in order to use these fluorescence yields to deduce ionization cross sections the spectra must be sufficiently resolved energetically that

TABLE II. K x-ray production cross sections: Ar^{q+} on Ne. Errors include the uncertainties in gas target pressure measurement and in x-ray counting, but do not include the uncertainty in detector window transmission estimates. The entries might be in error by as much as a factor of 2 for the lowest energy x rays due to the uncertainty in window transmission. For x rays near 3 keV, this uncertainty is reduced to 15%.

q	Neon (target)		Argon (projectile)	
	$\sigma_K \bar{\omega}_K$ (10^{-19} cm ²)		$\sigma_K \bar{\omega}_K$ (10^{-19} cm ²)	
	80 MeV	152 MeV	80 MeV	152 MeV
6	1.1±0.1	...	0.071±0.008	...
8	...	2.2±0.2	...	0.45±0.03
12	11±1	...	0.19±0.02	...
13	16±1	...	0.24±0.02	...
14	21±2	7.5±0.7	0.34±0.04	0.97±0.08
15	34±2	9.0±0.7	0.55±0.05	1.3±0.1
16	48±4	12±1	3.1±0.2	1.4±0.1
17	...	17±1	...	2.0±0.1
18	...	29±3	...	26±2

TABLE III. K x-ray production cross sections: Cl^{q+} on Ne. See Table II for an explanation of errors.

q	Neon (target)		Chlorine (projectile)	
	$\sigma_K \bar{\omega}_K$ (10^{-19} cm ²)		$\sigma_K \bar{\omega}_K$ (10^{-19} cm ²)	
	42 MeV	50 MeV	42 MeV	50 MeV
10	5.9±0.4	...	0.12±0.01	...
11	10±1	9.5±0.8	0.14±0.01	0.24±0.03
12	13±1	13±1	0.18±0.02	0.30±0.03
13	21±1	20±2	0.25±0.02	0.41±0.04
14	30±2	31±2	0.34±0.03	0.55±0.07
15	52±5	...	0.92±0.07	...

individual radiating configurations can be identified. Recently, some higher-resolution data have been published for selected collision systems^{10,11} using crystal spectrometers. Although these data provide more information as regards the multiplicity of target states produced than do Si(Li) data, they do not accurately reflect either the relative or absolute intensities of the various spectral features on account of the strongly energy dependent, and poorly known, solid-angle and crystal-reflectivity factors.

IV. DISCUSSION

Theories of inner-shell ionization by heavy charged particles apply separately to two types of collisions: Slow and fast, referring to whether or not the collision time is long or short, respectively, compared to an orbital period of the inner electron whose removal is being considered. One theoretical approach that is useful if the projectile velocity is slow compared to the orbital velocity of the inner-shell electron is to view the colliding system as a transient quasimolecule.¹² If the projectile L shell lies lower in energy than the target K shell, vacancies that exist in the L shell of the projectile prior to the collision can be transferred during a penetrating collision to the K shell of the (usually lighter) target atom. These vacancy transfers are thought to be enhanced when-

TABLE IV. Fluorine K x-ray production cross sections: 42-MeV Cl^{q+} on SF₆ (per molecule). See Table II for an explanation of errors.

q	$\sigma_K \bar{\omega}_K$ (10^{-19} cm ²)
10	4.6±0.5
11	7.0±0.6
12	8.0±0.7
13	14.0±1.0
14	28.0±2.0
15	82.0±8.0

TABLE V. Chlorine K x-ray production cross sections: 43-MeV F^{9+} on Freon (per molecule). See Table II for an explanation of errors.

q	$\sigma_K \bar{\omega}_K$ (10^{-19} cm 2)	
	$ClCF_3$	Cl_2CF_2
7	0.29 ± 0.02	0.50 ± 0.04
8	0.49 ± 0.04	0.91 ± 0.06
9	0.80 ± 0.05	1.5 ± 0.1

ever an energy level of one collision partner coincides approximately with a partially filled level of the other.

If these quasimolecular effects were of significant magnitude compared to other effects in our experiments we would expect to observe a resonance-like enhancement of the x-ray cross section as the vacancy-containing L shell of the Cl or Ar projectile is tuned, via adjustment of projectile charge, through the K shell of the Ne target. A log-log extrapolation of binding energy versus Z , based on published data¹³ on L -shell binding energies for the He, Li, Be, B, and C isoelectronic sequences indicates that the Ar^{14+} L shell lies ~ 20 eV lower than the Ne K shell.¹⁴ No such enhancement is observed (Fig. 1), probably because the projectile velocities used here are so high and the corresponding collision time is so short that the K -shell electrons in the target cannot respond quasiadiabatically to the changing perturbing field.

The plane-wave Born approximation (PWBA) treats the projectile as a point charge which ionizes the target via Coulomb excitation. As modified recently by Basbas, Brandt, and Laubert¹ this approximation should be valid for fast

collisions involving either fully stripped projectiles or ions whose electrons are weakly bound compared to those in the target K shell and for which $Z_{\text{projectile}} \ll Z_{\text{target}}$. Under these conditions the K -shell electron is influenced only by the nuclear charge of the projectile.

The projectiles used in the present experiments all travel at velocities which are of the same order of magnitude as the target K -shell electron velocity; that is, neither slow nor fast.

It therefore seems that even if we could reliably reduce our x-ray production cross sections to ionization cross sections, we could not meaningfully compare our results with theory because the projectiles' velocities do not satisfy the assumptions of the various theories. No theory exists which is adequate to describe the collision systems studied here. Nevertheless, we can compare our x-ray cross sections with those expected from a calculable although somewhat oversimplified model. First we compute the K shell ionization cross section $\sigma_{\text{ion}}^K(Z)$ for a fully stripped ion of nuclear charge Z , using either the PWBA¹ or the classical binary-encounter approximation (BEA), developed by Garcia² for protons and α particles. From these ionization cross sections it is possible to predict x-ray cross sections for those collisions which do not cause multiple ionization in the target, but leave the target with a single K -shell vacancy after the collision. We have made estimates of K x-ray cross sections based on these assumptions, and using recently compiled recommended fluorescence yields.¹⁵

Our estimates are listed in Table VI for five of the collisions studied. Experimental yields, even for ions in charge states which produce relatively

TABLE VI. Theoretical ionization and x-ray production cross sections for fully stripped projectiles.

Projectile	Energy/amu (MeV)	Target	u/v ^a	σ_K ^b (10^{-18} cm 2)	ω_K ^c σ_K ^b (10^{-20} cm 2)	σ_K ^d (10^{-18} cm 2)	ω_K ^c σ_K ^d (10^{-20} cm 2)
$^{40}_{18}Ar$	3.79	Ne	0.649	24.0	43.2	27.6	49.7
$^{40}_{18}Ar$	1.96	Ne	0.903	28.2	50.8	35.1	63.2
$^{35}_{17}Cl$	1.43	Ne	1.06	25.0	45.0	32.4	58.3
$^{35}_{17}Cl$	1.21	Ne	1.15	24.3	43.7	31.3	56.3
$^{19}_9F$	2.26	Cl	1.51	0.518	4.95	0.587	5.61

^a $u = (2u_K/m_e)^{1/2}$, $v = (2E/M)^{1/2}$ where u_K is the target K -shell binding energy (Ref. 14), m_e is the electron mass, E is the projectile energy, and M is the projectile mass.

^b Plane-wave Born approximation (e.g., Ref. 1, *without* modifications).

^c Fluorescence yield assumed to be that of atom with a single K -shell vacancy (Ref. 15).

^d Classical binary-encounter approximation as modified by Garcia (Ref. 2).

low yields, (Tables II-V) are an order of magnitude larger than the predictions using either PWBA or BEA. (The modified PWBA is not used here since the binding corrections contained in that modification are not valid for $Z_p \approx Z_T$.) The most unrealistic assumption in our model is the neglect of multiple ionization that is known to occur when heavy ions interact with gas targets.¹¹ This assumption underestimates the true fluorescence yield and therefore underestimates the x-ray cross section. For neon, at least, configurations of sufficiently large fluorescence yield to account fully for the disagreement between model and observation should radiate at energies⁹ measurably higher (40-100 eV) than the energies corresponding to the centroids in our spectra. It therefore seems highly likely that the target K-shell ioniza-

tion cross section itself is at least partially responsible for the projectile charge-state dependence of the target x-ray cross section.

ACKNOWLEDGMENTS

The authors are especially grateful for the encouragement and advice of Matt Brown and James Macdonald and for their valuable participation in one of our earlier experiments on this subject (Ref. 4). We also acknowledge useful discussions with Sheldon Datz, Rex Trammel (ORTEC), Patrick Richard, and Eugen Merzbacher. The technical assistance of M. B. Marshall and D. C. Hensley at ORIC was indispensable. We also acknowledge George Werner for assistance in setting up apparatus and taking data.

*Research supported in part by the National Aeronautics and Space Administration, by the Office of Naval Research, and by Union Carbide Corporation under contract with the U. S. Atomic Energy Commission.

¹For example, a completely quantum-mechanical treatment ("first" plane-wave Born approximation modified to include the perturbation of the target energy levels by the incoming projectile and the deflection of the projectile in the Coulomb field of the atomic nucleus) is given by George Basbas, Werner Brandt, and Roman Laubert, *Phys. Rev. A* **7**, 983 (1973); and Werner Brandt, in *Third International Conference on Atomic Physics, Boulder, Colorado* (Plenum, New York, 1973), p. 155.

²For example, a classical approach (binary-encounter approximation) is given by J. D. Garcia, *Phys. Rev. A* **1**, 1402 (1970); *Phys. Rev. A* **4**, 955 (1971); J. D. Garcia, R. J. Fortner, and T. M. Kavanagh, *Rev. Mod. Phys.* **45**, 111 (1973).

³J. R. Macdonald, L. M. Winters, M. D. Brown, L. D. Ellsworth, T. Chiao and E. W. Pettus, *Phys. Rev. Lett.* **30**, 251 (1973); G. Basbas, W. Brandt, R. Laubert, A. Ratkowski and A. Schwarzschild, *Phys. Rev. Lett.* **27**, 171 (1971); C. W. Lewis, R. L. Watson and J. B. Natowitz, *Phys. Rev. A* **5**, 1773 (1972). See also A. van der Woude, M. J. Saltmarsh, C. A. Ludemann, R. L. Hahn and E. Eichler, in *Proceedings of the International Conference on Inner Shell Ionization Phenomena, Atlanta, Georgia, 1973* (unpublished), p. 1388; C. W. Lewis, R. L. Watson, J. B. Natowitz, and T. L. Hardt, *ibid.* p. 1406.

⁴J. Richard Mowat, I. A. Sellin, D. J. Pegg, R. S. Peterson, Matt D. Brown, and James R. Macdonald, *Phys. Rev. Lett.* **30**, 1289 (1973). The apparent lack of signal

or noise in the lower 10 channels of Fig. 1 is a result of the pulse height discrimination setting, and not the result of a noiseless low-energy spectrum.

⁵James R. Macdonald, Loren Winters, Matt D. Brown, Tang Chiao, and Louis D. Ellsworth, *Phys. Rev. Lett.* **29**, 1291 (1972).

⁶Werner Brandt, Roman Laubert, Manuel Mourino, and Arthur Schwarzschild, *Phys. Rev. Lett.* **30**, 358 (1973).

⁷For a recent summary of photoionization cross sections in the energy range 0.1-1000 keV see W. J. Veigele, *At. Data Tables* **5**, 51 (1973).

⁸The gold layer is thought to possess a weblike structure, making its density nonuniform and its transmission much higher than that of a uniform layer of vacuum deposited gold. See J. M. Jaklevic and F. S. Goulding, *Trans. IEEE* **18**, 187 (1971).

⁹C. P. Bhalla, N. O. Folland and M. A. Hein, *Phys. Rev. A* **8**, 649 (1973).

¹⁰A. R. Knudson, D. J. Nagel, P. G. Burkhalter and K. L. Dunning, *Phys. Rev. Lett.* **26**, 1149 (1971); Patrick Richard, W. Hodge, and C. Fred Moore, *Phys. Rev. Lett.* **29**, 393 (1972).

¹¹R. L. Kauffman, F. Hopkins, C. W. Woods, and P. Richard, *Phys. Rev. Lett.* **31**, 621 (1973).

¹²M. Barat and W. Lichten, *Phys. Rev. A* **6**, 211 (1972).

¹³W. L. Wiese, M. W. Smith, and B. M. Glennon, *Atomic Transition Probabilities* (U.S. GPO, Washington, D.C., 1966).

¹⁴J. A. Bearden and A. F. Burr, *Rev. Mod. Phys.* **39**, 125 (1967).

¹⁵Walter Bambynek, Bernd Crasemann, R. W. Fink, H. U. Freund, Hans Mark, C. D. Swift, R. E. Price, and P. Venugopala Rao, *Rev. Mod. Phys.* **44**, 716 (1972).